Tuning of the graphene surface plasmon by the monolayer MoS_2*

CHEN Lei (陈磊), **ZHANG Liang** (张良), **XU Xiaofang** (许孝芳), **and LÜ Liu** (吕柳)**
School of Mechanic Engineering, Jiangsu University, Zhenjiang 212013, China

(Received 4 March 2021; Revised 7 May 2021)

We proposed a graphene based active plasmonic device by the introduction of graphene-MoS_2 heterostructures. The device was composed of a monolayer MoS_2 layer between the silicon substrate and periodically arranged graphene nanoribbon arrays. The finite-difference time domain (FDTD) method was used to analyze and compare the changes of the surface plasmon resonant wavelength and modulation depth (*MD*) in the two cases with and without MoS_2. It was found that all the parameters of the width, period and Fermi level of the graphene nanoribbons affect the surface plasmon resonant wavelength of the plasmonic device. The introduction of the monolayer MoS_2 can produce a redshift about 3 μm of the surface plasmon resonant wavelength, while the *MD* is basically unchanged. The redshift of the graphene surface plasmon resonant wavelength will provide application prospects for new active graphene plasmonic devices.

Document code: A **Article ID:** 1673-1905(2021)11-0646-5
DOI https://doi.org/10.1007/s11801-021-1025-2

Recently, graphene has been demonstrated to manipulate electromagnetic signals at deep sub-wavelength scale with ultrahigh field confinement due to its unique electronic band structures. Especially, graphene plasmon resonance can be tuned via gating, structure dimensions, electrostatic doping and through conventional plasmonics based on noble metals in the terahertz and infrared region[1]. Besides, people have realized many graphene plasmonic devices such as tunable graphene array filters, Bragg reflectors, waveguides and so on[2].

Two-dimensional (2D) layered transition-metal dichalcogenides have attracted considerable interest for their unique layer-number-dependent properties. The material of 2D MoS_2 has enormous potential in solar cell and photo-detector owning to its high carrier mobility and tunable band gap ranging from 1.8 eV of monolayer to 1.29 eV of multilayers or bulk[3] . In particular, the vertical integration of these 2D materials into van der Waals heterostructures opens up a new dimension for the design of functional optoelectronic devices, and many exciting physical phenomena can be observed[4]. Recently, the graphene-MoS_2 heterostructures have shown impressive characteristics such as high responsivity. ZHANG et al[5] found that the photodetector based on this graphene-MoS_2 heterostructure was able to reach a high photoresponsivity up to 10^7 A/W while maintaining its unique ultrathin character. Later on Xu et al[6] designed a new few-layer MoS_2-graphene heterostructure synthesized by a vertically layer-stacking method which has a large enhancement in photoresponsivity and detectivity. The interface coupling between the graphene and MoS_2 can generate new lattice vibration modes, interlayer hybridization and relativistic carriers[7]. Besides, the excitonic states in the MoS_2-graphene van der Waals heterostructures can be tuned via electrochemical gating, which was reported by LI et al[8]. They found that the photoluminescence intensity of the excitons (or trions) could be modulated by more than two orders of magnitude and the trion/exciton intensity ratio in MoS_2-graphene could be changed by up to 30 times. Besides, the hybrid graphene-MoS_2 surface plasmon resonant sensor possessed a phase-sensitive enhancement factor of more than 500-fold when compared to the sensing scheme with only graphene coating[9]. Moreover, the MoS_2-graphene heterostructures also showed superior practical advantages in the applications of memory cells[10], biomolecular detection[11] and lithium-ion battery anode materials[12].

In this paper, we proposed a graphene-based active plasmonic device structure by the introduction of the MoS_2-graphene heterostructures. Particularly, monolayer MoS_2 is placed between the graphene nanoribbon arrays and silicon substrate. We employed commercial finite-difference time domain (FDTD) solutions to analyze the influence of the monolayer MoS_2 on the surface plasmon resonant wavelength and modulation depth (*MD*) of the plasmonic device.

Fig.1 shows the schematic of the designed model. A

* This work has been supported by the National Natural Science Foundation of China (Nos.11204107 and 91750112).
** E-mail: lvliu@ustc.edu.cn

single layer of MoS_2 with thickness of 0.65 nm is placed uniformly on the silicon substrate, then covered by periodically arranged graphene nanoribbon arrays with a width α and period β. In order to control the conductivity of the graphene by the applied voltage, the p-type silicon is used as the bottom gate, while the two metal/graphene contacts are used as the drain and source electrodes, respectively. The surface plasmon of the graphene nanoribbon arrays was excited by normal incident plane waves. To investigate the effects of MoS_2 on the plasmonic device, the case of the remove of MoS_2 layer in the model of Fig.1 is also studied as a reference for comparison.

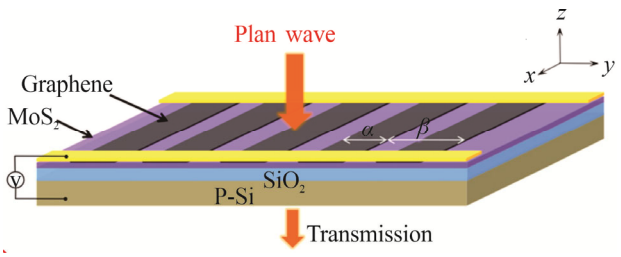

Fig.1 Schematic of the designed plasmonic device

The simulation of the surface plasmon resonant wavelength of the plasmonic device was carried out using FDTD solutions. The graphene in the simulation is a two-dimensional material without considering its thickness, which can speed up the simulation. The thickness of the monolayer MoS_2 is fixed at 0.65 nm. The overall mesh is 0.25 nm, but a local dense mesh of 0.01 nm is used for the graphene and MoS_2 portions. The boundary conditions in the Z direction are the perfect matching layer, while the other directions are applied with the periodic boundary conditions. The wavelength of the excitation light is tuned from 5 μm to 25 μm. Besides, the dielectric functions of the graphene and MoS_2 (semiconductor properties of the 2H phase) were taken respectively from Palik (1998)[13], and Hsu (2019)[14].

Fig.2 shows the transmission spectra of the plamonic device as a function of the width α and the period β of the graphene nanoribbon arrays. The occupation ratio is defined as α/β, which is kept at 50% for the simulation in Fig.2. As indicated by Fig.2, the surface plasmon can be perfectly excited by the designed plasmonic device, when the widths of the nanoribbons are 100 nm, 150 nm, and 200 nm. Besides, with the width α increased from 100 nm to 200 nm, the surface plasmon resonant wavelength redshifts from 17.00 μm to 22.48 μm, accompanied by the broadening of the transmission spectrum.

Fig.3(a) presents the variation of the surface plasmon resonant wavelength with the period β of the graphene nanoribbons arrays for the cases with and without MoS_2. The width α here is fixed at 150 nm in Fig.3(a). It can be seen that when β is increased from 200 nm to 500 nm, the surface plasmon resonant wavelength would blue-shift for the two cases. However, for the case with MoS_2, the blueshift range tends to be gradual, and the surface plasmon resonant wavelength has a red-shift of 3 μm as compared to the case without MoS_2. Fig.3(b) shows the variation of the surface plasmon resonant wavelength with the graphene nanoribbons width α. Here the period β is fixed at 300 nm. It can be observed that the surface plasmon resonant wavelength is redshifted with the increasing of the width α for the two cases. Moreover, the introduction of a single layer of MoS_2 in the plasmonic device would also lead to a redshift of the resonant wavelength about 3 μm. We attribute this phenomenon to the change of the dielectric constant of the graphene, which is alter from silica (ε_S=1.5) to MoS_2 (ε_M=5.48). As it is known, the resonant wavelength of the traditional surface plasmon of the metallic structure is greatly dependent on the dielectric environment of the metal. Similarly, as the reference reported[1], the plasmon wavelength of the graphene was also experimentally observed to be dependent on the dielectric constant of the SiC substrate.

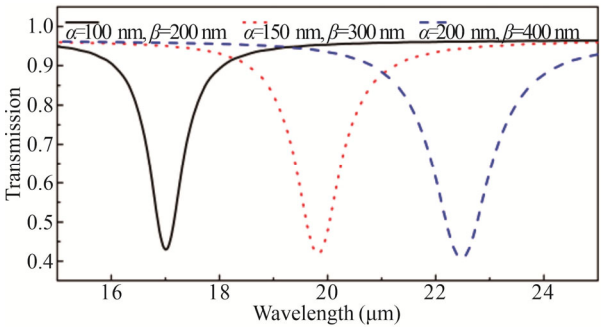

Fig.2 Transmission spectra with different ribbon widths with occupation ratio fixed at 50%

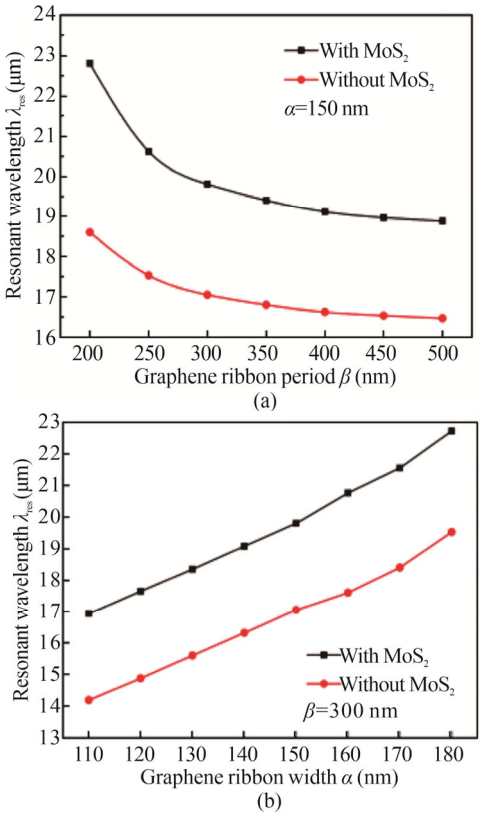

Fig.3 Variation of the resonant wavelength with the graphene nanoribbons (a) period and (b) width

OKANO et al[15] proved that the dielectric function of graphene can be modified in a broad spectral range by applying a back-gate voltage. Moreover, this special character contributes to actively control of the surface plasmon of the graphene, which results in many interesting phenomena. For example, YAO et al[16] demonstrated a spectrally and spatially tunable terahertz metasurface lens based on surface plasmons of graphene nanoribbons. The response frequency and the focal point of this lens can be dynamically modulated through varying the Fermi level of the graphene nanoribbons. As shown in Fig.4, the change of the surface plasmon resonant wavelength of the plasmonic device in this work with the Fermi level of the graphene was also studied. The width α and the period β are respectively fixed at 150 nm and 300 nm. It is obvious that with the increasing of the Fermi level of the graphene from 0.2 eV to 0.9 eV, the surface plasmon resonant wavelength in the cases with and without MoS_2 would blueshift about 10 μm. This phenomenon demonstrates that the plasmon wavelength is dependent on the Fermi level, and the reason can be described to that the change of the applied voltage on graphene would cause the change of the Fermi level E_f of the graphene, as well as the surface conductivity σ and the dielectric constant of the graphene.

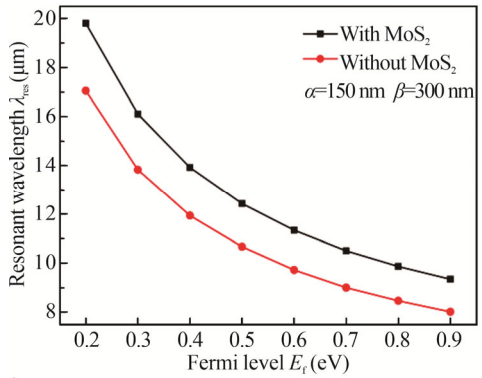

Fig.4 Variation of the resonant wavelength with Fermi level E_f

Besides the surface plasmon resonant wavelength, the *MD* is another factor to evaluate the properties of the plasmonic device. As Fig.4 indicated, the variation of Fermi level would cause the change of the resonant wavelength. Therefore, we can define the modulation depth as $MD=(E_{on}-E_{off})/E_{on}$[17]. Here, E_{on} and E_{off} are the surface plasmon resonant wavelength in the transmission spectrum, and corresponding to the "on" state (eg, E_f=0.25 eV) and the "off" state (eg, E_f=0.20 eV), respectively.

As shown in Fig.5, the graphene Fermi level is respectively adjusted between the four groups of values 0.20—0.25 eV, 0.40—0.45 eV, 0.60—0.65 eV, and 0.80—0.85 eV. As can be seen from the transmission spectra, when the Fermi level of the graphene increases, the transmission spectra become sharper. By contrasting the states of the “on” and “off”, the *MD* and the resonant wavelength shift $\Delta\lambda$ can be obtained from Fig.5. The obtained values of $\Delta\lambda$ and *MD* are respectively shown in

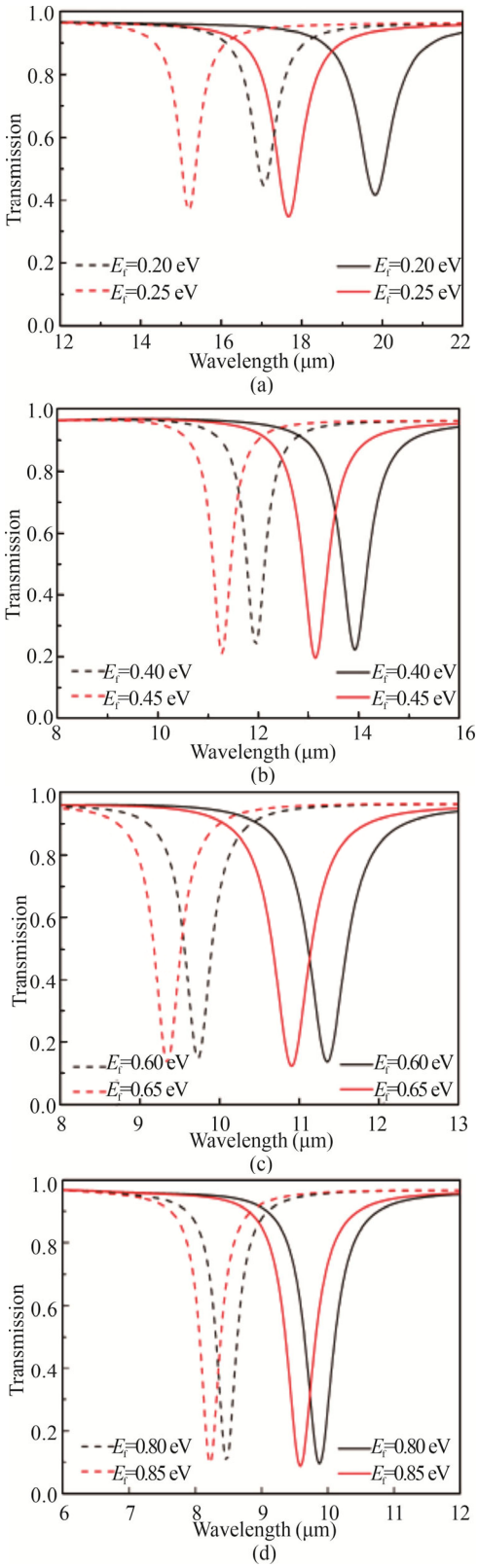

Fig.5 Transmission spectra for four groups of Fermi levels: (a) 0.20—0.25 eV; (b) 0.40—0.45 eV; (c) 0.60—0.65 eV; (d) 0.80—0.85 eV (The solid and dash lines are respectively corresponding to the cases with and without MoS_2.)

Fig.6(a) and (b). Obviously, the larger the Fermi level of the graphene increases, the smaller the corresponding $\Delta\lambda$ becomes. Moreover, $\Delta\lambda$ of the case with the MoS_2 is larger than that of the case without MoS_2. This phenomenon is more obvious when the Fermi level of the graphene decreases. Similarly, as shown in Fig.6(b), the *MD* decreases with the increasing of the Fermi level of the graphene. However, the effect of the MoS_2 on the *MD* is weak. Therefore, among the four sets of data, the Fermi level of the graphene between 0.20—0.25 eV has the maximum *MD*, as well as the maximum $\Delta\lambda$.

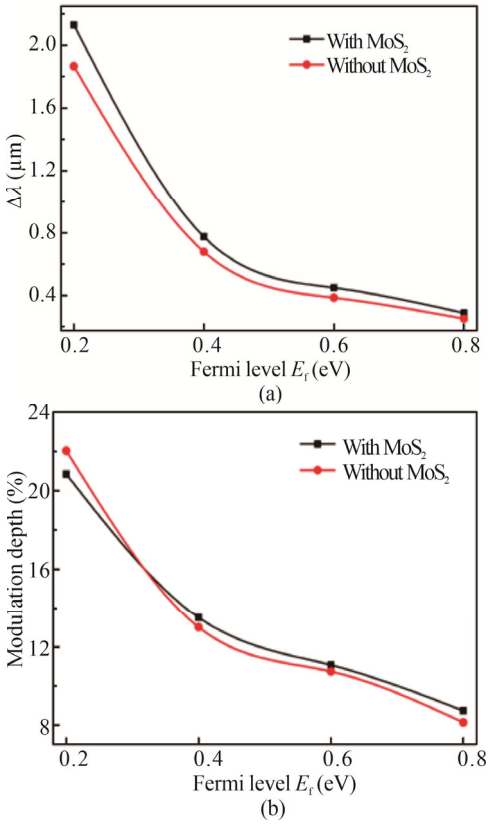

Fig.6 The changes of (a) $\Delta\lambda$ and (b) *MD* with the Fermi level of the graphene

We further studied the change of the *MD* and the $\Delta\lambda$ with the variation of the layer number *N* of the grapheme. As shown in Fig.7, it is clear that when the layer number of the graphene increases, the *MD* increases from approximately 20% to 85% for the cases with and without MoS_2. In addition, the increasing of the layer number of the graphene from 1 to 5 also causes a drop of the $\Delta\lambda$, which reaches 48.83% and 47.31% for the cases with and without MoS_2, respectively.

In conclusion, a graphene based active plasmonic device by the introduction of the graphene-MoS_2 heterostructures was proposed. The surface plasmon resonant wavelength of this plasmonic device could be adjusted by the width, period, Fermi level of the graphene nanoribbons arrays. Besides, the change of the *MD* and the $\Delta\lambda$ with the variation of the layer number *N* and the Fermi level of the graphene were also studied. It was found that

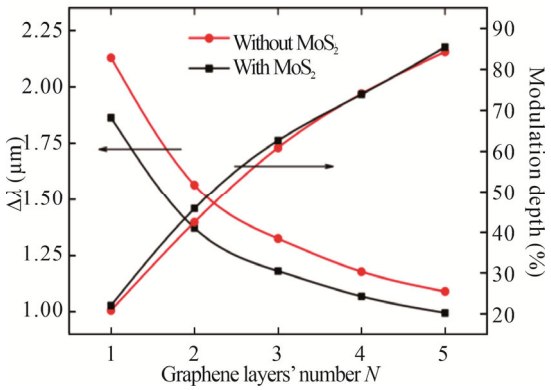

Fig.7 The changes of *MD* and $\Delta\lambda$ with the layer number *N* of the graphene

the presence of the MoS_2 layer not only causes the redshift of the surface plasmon resonant wavelength but also a larger of $\Delta\lambda$. The present work will provide application prospects for new active graphene plasmonic devices based on graphene-MoS_2 heterojunctions for the near infrared to terahertz band.

References

[1] CHEN J, BADIOLI M, ALONSO-GONZALEZ P, et al. Optical nano-imaging of gate-tunable graphene plasmons[J]. Nature, 2012, 487(7405): 77-81.

[2] FAN Y C, SHEN N H, ZHANG F L, et al. Graphene plasmonics: a platform for 2D optics[J]. Advanced optical materials, 2019, 7(13): 1800537.

[3] YANG X G, LI B J. Monolayer MoS_2 for nanoscale photonics[J]. Nanophotonics, 2020, 9(7): 1557-1577.

[4] WANG Y, JIN Y H, LI S B, et al. Flower-like MoS_2 supported on three-dimensional graphene aerogels as high-performance anode materials for sodium-ion batteries[J]. Ionics, 2018, 24(11): 3431-3437.

[5] ZHANG W J, CHUU C P, HUANG J K, et al. Ultrahigh-gain photodetectors based on atomically thin graphene-MoS_2 heterostructures[J]. Scientific reports, 2014, 4(1): 03826.

[6] XU H, HAN X Y, DAI X, et al. High detectivity and transparent few-layer MoS_2/glassy-graphene heterostructure photodetectors[J]. Advanced materials, 2018, 30(13): 1706561.

[7] LI H, WU J B, RAN F R, et al. Interfacial interactions in van der waals heterostructures of MoS_2 and graphene[J]. ACS nano, 2017, 11(11): 11714-11723.

[8] LI Y, XU C Y, QIN J K, et al. Tuning the excitonic states in MoS_2/graphene van der waals heterostructures via electrochemical gating[J]. Advanced functional materials, 2016, 26(2): 293-302.

[9] ZENG S W, HU S Y, XIA J, et al. Graphene-MoS_2 hybrid nanostructures enhanced surface plasmon resonance biosensors[J]. Sensors and actuators B: chemical, 2015, 207: 801-810.

[10] ROY K, PADMANABHAN M, GOSWAMI S, et al. Graphene-MoS_2 hybrid structures for multifunctional photoresponsive memory devices[J]. Nature nanotech-

nology, 2013, 8(11)：826-830.

[11] LOAN P T K, ZHANG W J, LIN C T, et al. Graphene/MoS_2 heterostructures for ultrasensitive detection of DNA hybridisation[J]. Advanced materials, 2014, 26(28)：4838-4844.

[12] WANG B B, ZHANG Y, ZHANG J, et al. Facile synthesis of a MoS_2 and functionalized graphene heterostructure for enhanced lithium-storage performance [J]. ACS appllied materials & interfaces, 2017, 9(15)：12907-12913.

[13] PRUCHA E J, PALIK E D. Handbook of optical constants of solids[M]. New York：Academic Press, 1998.

[14] HSU C W, FRISENDA R, SCHMIDT R, et al. Thickness-dependent refractive index of 1L, 2L, and 3L MoS_2, $MoSe_2$, WS_2, and WSe_2[J]. Advanced optical materials, 2019, 7(13)：1900239.

[15] OKANO S, SHARMA A, ORTMANN F, et al. Voltage-controlled dielectric function of bilayer graphene[J]. Advanced optical materials, 2020, 8(20)：2000861.

[16] YAO W, TANG L L, WANG J, et al. Spectrally and spatially tunable terahertz metasurface lens based on graphene surface plasmons[J]. IEEE photonics journal, 2018, 10(4)：1-8.

[17] CHU H S, GAN C. Active plasmonic switching at mid-infrared wavelengths with graphene ribbon arrays[J]. Applied physics letters, 2013, 102(23)：231107.